



TITLE:

Synthesis and biological activities of the amide derivative of aplog-1, a simplified analog of aplysiatoxin with anti-proliferative and cytotoxic activities.

AUTHOR(S):

Hanaki, Yusuke; Yanagita, Ryo C; Sugahara, Takahiro; Aida, Misako; Tokuda, Harukuni; Suzuki, Nobutaka; Irie, Kazuhiro

CITATION:

Hanaki, Yusuke ...[et al]. Synthesis and biological activities of the amide derivative of aplog-1, a simplified analog of aplysiatoxin with anti-proliferative and cytotoxic activities.. Bioscience, biotechnology, and biochemistry 2015, 79(6): 888-895

ISSUE DATE:

2015

URL:

<http://hdl.handle.net/2433/202083>

RIGHT:

This is an Accepted Manuscript of an article published by Taylor & Francis in 'Bioscience, biotechnology, and biochemistry' available online: <http://www.tandfonline.com/10.1080/09168451.2014.1002452>; The full-text file will be made open to the public on 23 Jan 2016 in accordance with publisher's 'Terms and Conditions for Self-Archiving'; この論文は出版社版ではありません。引用の際には出版社版をご確認ご利用ください。; This is not the published version. Please cite only the published version.

Synthesis and biological activities of the amide derivative of aplog-1, a simplified analog of aplysiatoxin with anti-proliferative and cytotoxic activities

Yusuke Hanaki,¹ Ryo C. Yanagita,^{1,2} Takahiro Sugahara,³ Misako Aida,³ Harukuni Tokuda,⁴ Nobutaka Suzuki,⁴ and Kazuhiro Irie*,¹

¹*Division of Food Science and Biotechnology, Graduate School of Agriculture, Kyoto University, Kyoto 606-8502, Japan*

²*Department of Applied Biological Science, Faculty of Agriculture, Kagawa University, Kagawa 761-0795, Japan*

³*Center for Quantum Life Sciences, and Department of Chemistry, Graduate School of Science, Hiroshima University, Higashi-Hiroshima 739-8526, Japan*

⁴*Department of Complementary and Alternative Medicine, Clinical R & D, Graduate School of Medical Science, Kanazawa University, Kanazawa 920-8640, Japan*

Received November 12, 2014; Accepted December 11, 2014

*Corresponding author. Tel.: +81-75-753-6281; fax: +81-75-753-6284; e-mail: irie@kais.kyoto-u.ac.jp

Abstract

Aplog-1 is a simplified analog of the tumor-promoting aplysiatoxin with anti-proliferative and cytotoxic activities against several cancer cell lines. Our recent findings have suggested that protein kinase C δ (PKC δ) could be one of the target proteins of aplog-1. In the present study, we synthesized amide-aplog-1 (**3**), in which the C-1 ester group was replaced with an amide group, to improve chemical stability *in vivo*. Unfortunately, **3** exhibited 70-fold weaker binding affinity to the C1B domain of PKC δ than that of aplog-1 and negligible anti-proliferative and cytotoxic activities even at 10⁻⁴ M. A conformational analysis and density functional theory calculations indicated that the stable conformation of **3** differed from that of aplog-1. Since 27-methyl and 27-methoxy derivatives (**1**, **2**) without the ability to bind to PKC isozymes exhibited marked anti-proliferative and cytotoxic activities at 10⁻⁴ M, **3** may be an inactive control to identify the target proteins of aplogs.

Key words: Aplysiatoxin, Anti-proliferative, Protein kinase C, Tumor promoter

Aplysiatoxin (ATX) is a potent tumor promoter that has been isolated from the digestive gland of the sea hare *Stylocheilus longicauda*.¹⁾ ATX strongly binds to and activates protein kinase C (PKC) isozymes, as well as 12-*O*-tetradecanoylphorbol 13-acetate (TPA) and teleocidin B-4.^{2,3)} Since PKC is a family of serine/threonine kinases that play pivotal roles in cellular signal transduction including proliferation, differentiation, and apoptosis,⁴⁻⁶⁾ tumor promoters may become therapeutic agents for intractable diseases such as cancer, Alzheimer's disease (AD), and acquired immune deficiency syndrome (AIDS). However, difficulties are associated with their application to therapeutic uses due to their potent tumor-promoting and inflammatory activities.^{7,8)}

Bryostatin-1 (bryo-1)⁹⁾ which was isolated from the marine bryozoan *Bugula neritina*, is a unique PKC activator that does not exhibit tumor-promoting or inflammatory activity. Bryo-1 has been reported to have significant anti-cancer and anti-proliferative activities, and these have been attributed to activation of the PKC δ [] [] [] [] [] [] []¹⁰⁻¹²⁾ which plays a tumor suppressor role and is involved in apoptosis.¹³⁻¹⁵⁾ Bryo-1 is also expected to become a therapeutic candidate for AD¹⁶⁾ and AIDS.¹⁷⁾ Despite its potential as a new medicinal lead, further studies on its mode of action and structural optimization have been hampered due to its limited availability from natural sources and synthetic complexity. A functional oriented synthesis of the simplified analogs of bryo-1 was recently conducted address these issues.^{18,19)}

As an alternative approach, we developed aplog-1, a simplified analog of ATX.²⁰⁾ Aplog-1, supplied in only 27 steps *via* standard reactions, was not tumor-promoting or inflammatory, but was anti-proliferative even though it has the skeleton of tumor-promoting ATX. The anti-proliferative activity of aplog-1 against several cancer cell lines was previously shown to be similar to that of bryo-1.²⁰⁾ Furthermore, aplog-1 behaved in a similar manner to bryo-1 rather than TPA for the translocation of GFP-tagged PKC δ using CHO-K1 cells; aplog-1 as well as bryo-1 translocated GFP-tagged PKC δ to the nuclear membrane and perinuclear region rather than to the plasma membrane, unlike TPA.²⁰⁾ To examine the contribution of PKC δ to the anti-proliferative activity of aplog-1, we recently synthesized 27-methyl and 27-methoxy derivatives (**1**, **2**) that lacked the ability to bind to PKC δ and evaluated their anti-proliferative activities against 39 human cancer cell lines.²¹⁾ Compounds **1** and **2** only exhibited weak anti-proliferative activities against all the human cancer cell lines tested,²¹⁾ suggesting that the activation of PKC δ was involved in growth inhibitory activities against

several cancer cell lines that were at least sensitive to aplog-1.

The next step is to evaluate and improve the anti-proliferative activity of aplog-1 *in vivo*. When a bioactive compound is applied to *in vivo* studies, its chemical stability is critical to the drug efficacy. Compounds with ester groups are generally susceptible to hydrolysis by esterases *in vivo*. For example, epothilone B²²⁾ showed cytotoxicity by inhibiting the depolymerization of microtubules²³⁾, but its efficacy was limited *in vivo* due to its ester group. Ixabepilone is a derivative of epothilone B, in which the ester group is replaced with an amide group. Ixabepilone was approved as an anti-breast cancer agent because of its potent cytotoxicity *in vivo*.^{24,25)} Aplog-1 has two ester linkages at C-1 and C-24 in the macrolactone ring. We previously reported that benzolactams, the simplified analogs of teleocidins, bound to PKC isozymes more strongly than their lactone counterparts, benzolactones,^{26,27)} which prompted us to develop a new derivative of aplog-1 with a more stable amide linkage. We herein described the synthesis of amide-aplog-1 (**3**), in which the ester group at C-1 of aplog-1 was replaced with an amide group, along with several of its biological activities such as PKC δ binding, *in vitro* tumor-promoting, anti-proliferative, and cytotoxic activities. We chose to replace the C-1 ester group because this site and benzolactones (Figure 1) share a common hydrophilic substructure, -C(=O)-O-CHR-CH₂OH, with an inversed stereochemistry, and the amide proton of **3** was expected to be at a spatial position similar to that of the hydrogen atom in the hemiacetal 3-OH group of ATX.

Results and Discussion

The synthesis of **3** was accomplished in a convergent approach from a spiroketal (**6**)²⁰⁾ and carboxylic acid (**5**), as shown in Scheme 1. Compound **4** was prepared from Z-D-Asp(O*t*Bu)-OH as reported previously²⁸⁾ and the subsequent removal of the *t*-butyl ester with trifluoroacetic acid (TFA) afforded the carboxylic acid (**5**). The spiroketal **6** was synthesized from *m*-hydroxycinnamic acid in a similar manner to the synthesis of aplog-1.²⁰⁾ Yamaguchi's esterification²⁹⁾ of **6** with **5** provided **7**. Oxidative cleavage of the olefin group, followed by esterification with *N*-hydroxysuccinimide, gave an activated ester. Immediately after deprotection of the benzyl (Bn) and carbobenzyloxy (Cbz) groups by catalytic hydrogenation, lactamization occurred to give **3** in a single step. The yield (23% in two steps) was not good because the Bn group resisted the catalytic hydrogenation.

We initially evaluated the ability of **3** to bind to PKC δ using a synthetic PKC δ -C1B peptide (δ -C1B),³⁰⁾ which is a major binding site and plays a predominant role in the activation

of PKC δ by PKC ligands such as bryo-1, ATX, and TPA. The concentration required to cause 50% inhibition (IC_{50}) of [3H]phorbol 12,13-dibutyrate (PDBu) was measured using a competitive binding assay.^{31,32)} Affinity for δ -C1B was expressed as a K_i value calculated from the IC_{50} value of **3** and the K_d value of [3H]PDBu, as reported by Sharkey and Blumberg.³¹⁾ Table 1 lists the K_i value of **3** for δ -C1B along with those of aplog-1 and its 27-methyl and 27-methoxy derivatives (**1** and **2**). As previously reported,^{21,33)} the stereochemistry at position 27 was critical for PKC binding, and the free hydroxyl group at position 27 was indispensable. Although the amide analog **3** fulfilled these structural requirements at position 27 for PKC δ binding, the affinity of **3** (K_i = 520 nM) was approximately two orders of magnitude weaker than that of aplog-1 (K_i = 7.4 nM).

Regarding PKC activators such as 1,2-diacyl-*sn*-glycerol (DAG) and indolactam-V (Fig. 1), the replacement of an ester group with an amide group and *vice versa* significantly affected their abilities to bind to PKC isozymes by changing their conformation. The replacement of either the *sn*-1 or *sn*-2 ester group of DAG, an endogenous second messenger, with an amide group markedly reduced its ability to activate PKC isozymes.³⁴⁾ The conformationally constrained analogs of DAG (DAG-lactones) with similar modifications developed by Marquez and colleagues also showed approximately ninety to two hundred-fold lower binding affinities for PKC α than those of their ester counterparts.³⁵⁾ On the other hand, amide-to-ester modification in the indolactam-V analogs gave opposite results. A lactone analog of the nine-membered indolactam-V, the core structure of teleocidins, showed a different conformational preference and was completely inactive,³⁶⁾ while a lactone analog of the eight-membered benzolactam-V8 took a ring conformation similar to that of benzolactam-V8 with *cis*-amide, and exhibited twenty to ninety-fold lower affinity for PKC C1 domains than the corresponding benzolactam-V8 analog.²⁷⁾ Therefore, both ester and amide analogs could bind to PKC isozymes if it adopted an appropriate conformation.

The strong binding ability of ATX to PKC isozymes was attributed to the rigid conformation of the macrocyclic ring, which included a hydrophilic pharmacophore,³³⁾ and an NMR analysis of aplog-1²⁰⁾ indicated that its preferred macrocyclic ring conformation was similar to that of 3-deoxy-debromo-ATX (*e.g.*, $J_{2,3}$ = 10.8 and 2.8 Hz for aplog-1; 11 and 3 Hz for 3-deoxy-debromo-ATX).³³⁾ In the case of **3**, an nOe correlation between NH-26 and H-11 was observed in a 2D NOESY NMR experiment in CDCl₃ (Supplemental Fig. 2), suggesting that the conformation of **3** differed to those of ATX³³⁾ and aplog-1, in which the distance between these atoms could be more than 4 Å. Since ATX and aplogs were involved in the

hydrophobic environment when bound to PKC δ -C1B in the presence of phosphatidylserine, the conformation of **3** in CDCl₃ would reflect a conformation in a ternary complex of **3**, PKC δ -C1B, and phosphatidylserine membrane. In order to clarify the effects of conformational changes in **3** on decreases in PKC δ binding, we performed a conformational search followed by density functional theory (DFT) calculations to estimate the relative stabilities of possible conformers.

A set of possible conformations of the macrolactone core structure of **3** was generated by the simulated annealing method, and we chose three possible conformers: the global-minimum with a *trans*-amide, an ATX-like conformation with a *trans*-amide, and a conformation with a *cis*-amide because the active conformation of indolactam compounds is known to be a *cis*-amide form.^{37,38)} Side chains at C-11 were attached to them and dihedral angles in the side chain were manually rotated to search for an energetically stable orientation, in which the 18-OH group is involved in intramolecular hydrogen bonding as suggested by its sharp ¹H NMR signal in CDCl₃. The candidate structures were pre-optimized using the molecular mechanics method with the MMFF94s force field and the final DFT geometry optimizations were then performed at the ω B97X-D/6-31G* level of theory.³⁹⁾ Figure 2 shows the resulting three possible conformers of **3** (A-C) and their relative ω B97X-D/6-31G* energies.

As described above, conformers **A** and **B** had a *trans*-amide bond, while **C** had a *cis* one. Conformer **B** resembles a stable conformation of ATX.³³⁾ In conformers **A** and **B**, NH-26 and H-11 were spatially close (2.06 Å in **A**, 2.61 Å in **B**), which is consistent with the nOe correlation. Furthermore, the sharp and downfield-shifted ¹H NMR signal of NH-26 (7.45 ppm) in CDCl₃ could be explained by intramolecular hydrogen bonding between N-H and an oxygen atom in these conformers. DFT calculations showed that conformer **A** had the lowest energy, and differences in energies between **A-B** and **A-C** were 1.365 and 13.259 kcal mol⁻¹, respectively. These results suggested that **3** existed as conformer **A** in CDCl₃. Since conformer **B** resembled but significantly diverged from the stable conformation of ATX due to the rotation of amide plane by 45° (based on N—C-1—C-2—C-3 dihedral angle), the difference in energies between conformer **A** and the ATX-like active conformation would be more than 1.365 kcal mol⁻¹. Thus, a 70-fold decrease in the binding ability of **3** from aplog-1, which is equivalent to a 2.34 kcal mol⁻¹ change in free energy, could be ascribable mainly to the change in the conformational preference.

We then evaluated the tumor-promoting activity of **3** *in vitro* by testing the induction of Epstein-Barr virus early antigen (EBV-EA) production.^{40,41)} EBV is activated by treating cells with tumor promoters such as TPA in order to produce EA, which can be detected by an indirect

immunofluorescence technique. Aplog-1 and its C-27 derivatives (**1** and **2**) induced EA production more weakly than the potent tumor promoter TPA. The ability of **3** to induce EA production was weaker than those of **1** and **2** without the ability to bind to PKC isozymes^{21,33)} (Figure 3). Although EA production is considered to be related to the activation of PKC isozymes,⁴²⁾ this result suggested that some part of the induction of EA caused by aplog-1 and its derivatives could be attributed to other mechanisms.

The anti-proliferative activity of **3** was evaluated with a panel of 39 human cancer cell lines established by Yamori and colleagues^{44,45)}. The results for HBC-4 and NCI-H460 were shown in Figure 4 as typical examples, because aplog-1 showed stronger growth inhibitory activity against these cell lines. Similar results were observed in MDA-MB-231, SNB-78, HCC2998, A549, LOX-IMVI, and St-4 cell lines (Supplemental Table 1). Cell growth was estimated by the sulforhodamine B assay and expressed as a percentage of the control without **3**. As expected from the weak binding affinity for PKC δ , **3** hardly inhibited their growth at low concentrations ($< 10^{-5}$ M) as well as **1** and **2**. Furthermore, **3** exhibited weak cytotoxicity even at 10^{-4} M, whereas aplog-1, **1**, and **2** induced cell death regardless of their binding affinities for PKC δ at the same concentration (10^{-4} M). This result suggests that other targets may be involved in the cytotoxicity of aplogs at 10^{-4} M.

In summary, we synthesized a new amide derivative of aplog-1 (**3**) in order to improve the stability of aplog-1 against esterases and pH changes *in vivo*. Although the very weak binding of **3** to the C1B domain of PKC δ could be detected, **3** showed weak anti-proliferative activity against the 39 cancer cell lines examined, even at 10^{-4} M (Supplemental Table 1), and hardly induced the production of EBV-EA. In contrast, aplog derivatives without binding affinity to PKC δ and its isozymes (**1**, **2**)²¹⁾ retained these activities at 10^{-4} M. These results suggest that some of the anti-proliferative and cytotoxic activities of aplogs were attributed to unidentified targets other than PKC isozymes. A conformational analysis and DFT calculations indicated that the stable conformation of **3** differed from that of aplog-1. This conformational change could prevent **3** from binding to PKC δ and other target proteins responsible for anti-proliferative activity and EBV-EA induction. Given that conformational changes in PKC ligands could affect not only biological activities, but also cellular targets, these effects must be taken into account to successfully derivatize the skeletons of aplogs in the future.

We recently developed aplog-based molecular probes and are currently attempting to identify its target proteins other than PKC isozymes. As described above, 27-methyl and

27-methoxy derivatives (**1**, **2**) did not exhibit the ability to bind to PKC isozymes, but had marked anti-proliferative and cytotoxic activities at 10^{-4} M, indicating that **1** and **2** were not suitable as inactive controls for the target analysis. Since **3** exhibited weak binding affinity for PKC, but little cytotoxic activity even at 10^{-4} M, it would be suitable as an inactive control for the identification of targets other than PKC isozymes.

Experimental

The following spectroscopic and analytical instruments were used: digital polarimeter, DIP-1000 (Jasco, Tokyo, Japan); ^1H and ^{13}C NMR, Avance III 400, Avance III 500, and Avance II 800 (reference TMS, Bruker, Germany); HPLC, model 600E with a model 2487 UV detector (Waters, Tokyo, Japan); and HR-FAB-MS, JMS-600H (JEOL, Tokyo, Japan) and JMS-700 (JEOL, Tokyo, Japan). HPLC was carried out on a YMC-packed ODS-A AA12S05-2510WT (Yamamura Chemical Laboratory, Kyoto, Japan). Wakogel® C-200 (silica gel, Wako Pure Chemical Laboratory, Osaka, Japan) was used for column chromatography. $[\text{}^3\text{H}]\text{PDBu}$ (18.7 Ci/mmol) was custom-synthesized by Perkin-Elmer Life Sciences Research Products (Boston, MA). The PKC δ C1B peptide was synthesized as reported previously.³⁰ All other chemicals and reagents were purchased from chemical companies and used without further purification.

Synthesis of 3. Compound **4** was prepared as reported previously.²⁸ $[\alpha]_{\text{D}} +13.2^\circ$ ($c = 0.44$, MeOH, 10.9°C). TFA (0.9 mL) was added to a solution of **4** (35.8 mg, 89.7 μmol) in dichloromethane (0.9 mL) at 0°C . After 4 h of stirring at room temperature, the reaction mixture was concentrated *in vacuo* to afford **5** (29.3 mg, 85.4 μmol , 95%) as a clear oil. ^1H NMR (500 MHz, CDCl_3 , 0.015 M) ppm: δ 2.70 (2H, d, $J = 5.9$ Hz), 3.55-3.59 (2H, m), 4.23 (1H, br. s), 4.50 (2H, s), 5.09 (2H, s), 5.41 (1H, br. d, $J = 8.1$ Hz), 7.27-7.37 (10H, m); ^{13}C NMR (125 MHz, CDCl_3 , 0.015 M) ppm: δ 35.8, 47.8, 66.9, 70.8, 73.4, 127.7 (2C), 127.9 (2C), 128.1, 128.2, 128.5 (2C), 128.6 (2C), 136.4, 137.7, 155.9, 174.1; HR-EI-MS m/z : 343.1427 ($[\text{M}]^+$ Calcd. for $\text{C}_{19}\text{H}_{21}\text{NO}_5$ 343.1420) $[\alpha]_{\text{D}} +16.1^\circ$ ($c = 0.15$, CHCl_3 , 10.3°C).

2,4,6-trichlorobenzoyl chloride (28.0 μL , 179 μmol , 1.7 equiv.) was added to a solution of **5** (51.1 mg, 149 μmol , 1.4 equiv.) and Et_3N (24.9 μL , 179 μmol , 1.7 equiv.) in toluene (1.1 mL) at room temperature. After 3 h of stirring at room temperature, the supernatant of the suspension was added to a solution of **6**²⁰ (50.0 mg, 105 μmol) and DMAP (27.0 mg, 221 μmol ,

2.1 equiv.) in toluene (1.1 mL) at room temperature. The mixture was stirred at 50 °C for 2 h and then poured into H₂O (5.0 mL). The mixture was extracted with EtOAc (5 mL x 3). The combined organic layers were washed with brine, dried over Na₂SO₄, filtered, and concentrated *in vacuo*. The residue was purified by column chromatography (silica gel, 10% → 20% EtOAc/hexane) to afford **7** (67.8 mg, 84.4 μmol, 80%) as a clear oil. ¹H NMR (500 MHz, CDCl₃, 0.0027 M) ppm: δ 0.86 (3H, s), 0.95 (3H, s), 1.33-1.49 (9H, m), 1.57-1.66 (4H, m), 2.19 (1H, br. d, *J* = 15.5 Hz), 2.26 (1H, m), 2.35 (1H, m), 2.57 (2H, t, *J* = 7.8 Hz), 2.61 (1H, dd, *J* = 15.8, 8.0 Hz), 2.69 (1H, dd, *J* = 5.8 Hz), 3.49-3.60 (4H, m), 4.16-4.21 (2H, m), 4.47-4.52 (2H, m), 4.95-5.02 (2H, m), 5.04 (2H, s), 5.06-5.09 (3H, m), 5.56 (1H, br. d, *J* = 8.8 Hz), 5.80 (1H, m), 6.78-6.82 (3H, m), 7.18 (1H, t, *J* = 7.8 Hz), 7.27-7.45 (14H, m); ¹³C NMR (125 MHz, CDCl₃, 0.0027 M) ppm: δ 22.0, 24.8, 25.3, 26.1, 27.2, 31.3, 33.7, 34.5, 35.6, 36.0, 36.5, 36.8, 40.9, 48.0, 63.9, 66.7, 68.4, 70.0, 71.1, 71.7, 73.3, 100.1, 111.8, 115.2, 116.6, 121.2, 127.5 (2C), 127.6 (2C), 127.8, 127.9 (2C), 128.1, 128.1, 128.4 (2C), 128.5 (2C), 128.6 (2C), 129.2, 135.4, 136.6, 137.3, 137.9, 144.6, 155.8, 158.9, 171.3; HR-FAB-MS (matrix, *m*-nitrobenzyl alcohol) *m/z*: 826.4324 ([M+Na]⁺ Calcd. for C₅₀H₆₁NO₈Na 826.4295) [α]_D +19.7° (*c* = 0.14, CHCl₃, 28.9 °C).

KMnO₄ (13.1 mg, 83.2 μmol, 1 equiv.) was added to a suspension of NaIO₄ (143 mg, 0.666 mmol, 8 equiv.) in pH 7.2 phosphate buffer (6.9 mL) in one portion. After 5 min of stirring at room temperature under an Ar atmosphere, the mixture was added to a solution of **7** (66.8 mg, 83.2 μmol) in *t*-BuOH (6.9 mL). The reaction mixture was stirred at room temperature for 1 h, and the reaction was quenched with Na₂S₂O₃ (39.5 mg). The organic layer was separated, and the aqueous layer was extracted with EtOAc (20 mL x 3). The combined organic layer were washed with brine, dried over Na₂SO₄, filtered, and concentrated *in vacuo*. The residue was purified by column chromatography (silica gel, 20% EtOAc/hexane containing 1% AcOH) to afford a carboxylic acid (50.8 mg, 61.9 μmol, 74%) as a clear oil.

N,N'-dicyclohexylcarbodiimide (7.3 mg, 35.4 μmol, 1.5 equiv.) in MeCN (0.20 mL) was added to a solution of the carboxylic acid (19.4 mg, 23.6 μmol) and *N*-hydroxysuccinimide (5.4 mg, 47.2 μmol, 2 equiv.) in MeCN (0.20 mL) at 0 °C. The reaction mixture was stirred at 0 °C for 10 h, then concentrated *in vacuo*. The residue was purified by column chromatography (silica gel, 5% → 10% → 20% → 30 % EtOAc/hexane) to afford a crude activated ester (28.1 mg). A solution of the activated ester (26.7 mg) in MeOH (1.0 mL) was added to 20% Pd(OH)₂-C (wet support, Aldrich) (7.8 mg) in a flask at room temperature. The mixture was vigorously stirred under a H₂ atmosphere at room temperature for 4.5 h. The mixture was

filtered and the filtrate was concentrated *in vacuo*. The residue was dissolved in MeOH (0.6 mL), and again added to 20% Pd(OH)₂-C (wet support, Aldrich) (5.9 mg) in a flask at room temperature. The mixture was vigorously stirred under a H₂ atmosphere at room temperature for 2.5 h. The mixture was filtered and the filtrate was concentrated *in vacuo*. This procedure was repeated two times and a total of 38.5 mg (46.9 μmol) of the carboxylic acid was reacted. These residues were purified by HPLC (column, YMC-Pack ODS-AA12S05-2510WT; solvent MeOH/H₂O = 75:25, flow rate 3.0 mL/min; pressure, 2100 psi; UV detector 254 nm; retention time, 20.1 min) to afford **3** (5.2 mg, 10.6 μmol, 23%) as a clear oil. ¹H NMR (400 MHz, CDCl₃, 0.0036 M) ppm: δ 0.96 (3H, s, H₃-23), 1.00 (3H, s, H₃-22), 1.38-1.59 (9H, m, H₂-4, H₂-5, H-10a, H₂-12, H₂-13), 1.64 (2H, m, H₂-14), 1.71 (1H, dd, *J* = 15.5, 3.7 Hz, H-8α), 1.79 (1H, m, H-10b), 2.28 (1H, dd, *J* = 15.1, 1.1 Hz, H-2a), 2.46 (1H, m, H-8β), 2.55-2.65 (4H, m, H-2b, H₂-15, H-25a), 2.95 (1H, dd, *J* = 16.5, 10.7 Hz, H-25b), 3.70-3.87 (4H, m, H-3, H-26, H₂-27), 4.09 (1H, m, H-11), 4.45 (1H, dd, *J* = 7.6, 5.0 Hz, OH), 5.21 (1H, m, H-9), 6.27 (1H, s, Ph-OH), 6.65-6.74 (3H, m, H-17, H-19, H-21), 7.13 (1H, t, *J* = 7.8 Hz, H-20), 7.45 (1H, br. d, *J* = 4.7 Hz, NH); ¹³C NMR (125 MHz, CDCl₃, 0.0029 M) ppm: δ 21.5 (C-22), 24.2 (C-13), 25.6 (C-8), 25.9 (C-23), 27.8 (C-4), 30.2 (C-14), 34.2 (C-5 or 10 or 12), 34.4 (C-5 or 10 or 12), 34.7 (C-5 or 10 or 12), 35.3 (C-15), 36.3 (C-25), 37.3 (C-6), 43.8 (C-2), 51.6 (C-26), 63.9 (C-11), 64.5 (C-27), 68.5 (C-9), 71.3 (C-3), 101.3 (C-7), 112.8 (C-19), 115.1 (C-17), 120.6 (C-21), 129.4 (C-20), 144.4 (C-16), 156.3 (C-18), 170.3 (C-24), 173.4 (C-1); HR-FAB-MS (matrix, *m*-nitrobenzyl alcohol) *m/z*: 490.2812 ([M+H]⁺ Calcd. for C₂₇H₄₀NO₇ 490.2805) [α]_D +38.9° (*c* = 0.074, CHCl₃, 9.6 °C).

Inhibition of specific binding of [³H]PDBu to the PKCδ-C1B peptide. The binding of [³H]PDBu to the δ-C1B peptide was evaluated by the procedure of Sharkey and Blumberg³¹⁾ with modifications as reported previously³²⁾ using 50 mM Tris-maleate buffer (pH 7.4 at 4 °C), 13.8 nM δ-C1B peptide, 20 nM [³H]PDBu (18.7 Ci/mmol), 50 μg/mL 1,2-dioleoyl-*sn*-glycero-3-phospho-L-serine sodium salt (Sigma), 3 mg/mL bovine γ-globulin, and various concentrations of an inhibitor. Binding affinity was evaluated based on the concentration required to inhibit the specific binding of [³H]PDBu by 50%, the IC₅₀, which was calculated by a computer program with a probit procedure.⁴⁶⁾ The inhibition constant, *K_i*, was calculated by the method of Sharkey and Blumberg.³¹⁾

EBV-EA induction test. Human B-lymphoblastoid Raji cells (5 × 10⁵/mL) were incubated at

37 °C under a 5% CO₂ atmosphere in 1 mL of RPMI 1640 medium (supplemented with 10% fetal bovine serum) with 4 mM sodium *n*-butyrate (a synergist) and 10, 100, or 1000 nM of each test compound. Each test compound was added as 2 μL of a DMSO solution (5, 50, and 500 μM stock solution) along with 2 μL of DMSO; the final DMSO concentration was 0.4%. After 48 h of incubation, smears were made from the cell suspension, and the EBV-EA-expressing cells were stained by a conventional indirect immunofluorescence technique with the serum of an NPC patient's (a gift from Kobe University, Japan) and FITC-labeled anti-human IgG (DAKO, Glostrup, Denmark) as reported previously.⁴¹⁾ At least 500 cells were counted in each assay and the proportion of EA-positive cells was recorded. Cell viability exceeded 60% in all experiments.

Measurements of cell growth inhibition. A panel of 39 human cancer cell lines established by Yamori and colleagues⁴⁴⁾ according to the NCI method with modifications was employed, and cell growth inhibitory activity was measured as reported previously.⁴⁵⁾ In brief, cells were plated on 96-well plates in RPMI 1640 medium supplemented with 5% fetal bovine serum and allowed to attach overnight. The cells were incubated with each test compound for 48 h. Cell growth was estimated by the sulforhodamine B assay. Absorbance for the control well (C) and test well (T) was measured at 525 nm along with that for the test well at time 0 (*T*₀). Cell growth inhibition (% growth) by each concentration of the drug (10⁻⁸, 10⁻⁷, 10⁻⁶, 10⁻⁵, and 10⁻⁴ M) was calculated as 100[(*T* - *T*₀)/ (*C* - *T*₀)] using the average of duplicate points.

Conformational search of 3. The generation of a conformer library of **3** by a simulated annealing method under a vacuum was performed using the GROMACS program⁴⁷⁾ (version 4.6.5) with a general AMBER force field (GAFF).⁴⁸⁾ The side chain at C11 of **3** was replaced with a methyl group. All bonds were constrained using the LINCS algorithm. The annealing temperature was initially set to 1,500 K in order to surpass the *cis-trans* isomerization barrier in this system and the temperature was kept constant for 1 ps. The temperature was linearly dropped to 100 K over 1 ps and then to 0 K over 1 ps, and kept at the same temperature for 1 ps. This 5-ps cycle was repeated 200 times to give the conformer library.

Three possible conformers were selected from this library: the global-minimum with *trans*-amide, ATX-like conformation with *trans*-amide, and a conformation with *cis*-amide. The side chains at C-11 were attached to them and dihedral angles in the side chain were manually rotated to search for energetically stable orientation. The candidate structures were

pre-optimized using the molecular mechanics method with the MMFF94s force field as implemented in Avogadro⁴⁹⁾ (version 1.1.1) and then optimized using the DFT method at the level of ω B97X-D/6-31G*³⁹⁾ employing Gaussian09.⁵⁰⁾ The obtained geometries were characterized as minimum structures on the basis of their harmonic vibrational frequencies and number of imaginary frequencies.

Acknowledgments

We thank the Screening Committee for Anticancer Drugs supported by a Grant-in-Aid for Scientific Research on Innovative Areas (“Scientific Support Programs for Cancer Research”) from the Ministry of Education, Culture, Sports, Science and Technology, Japan.

Mass measurements were partly carried out with the JEOL JMS-700 MS spectrometer in the joint Usage/Research Center (JURC) at the Institute for Chemical Research, Kyoto University, Japan. The DFT calculations were carried out at the Research Center for Computational Science, Okazaki National Research Institutes. The NOESY spectrum of **3** was measured by Dr. Ken-ichi Akagi at the National Institute of Biomedical Innovation (Osaka).

Funding

This work was partly supported by the Ministry of Education, Culture, Sports, Science and Technology, Japan under a Grant-in-Aid for Scientific Research on Innovative Areas “Chemical Biology of Natural Products” [number 23102011] (to KI and RCY), [number 26102733] (to MA).

References

- [1] Kato Y, Scheuer PJ. Aplysiatoxin and debromoaplysiatoxin, constituents of the marine mollusk *Stylocheilus longicauda* (Quoy and Gaimard, 1824). J. Am. Chem. Soc. 1974;96:2245–2246.
- [2] Kikkawa U, Takai Y, Tanaka Y, Miyake R, Nishizuka Y. Protein kinase C as a possible receptor protein of tumor-promoting phorbol esters. J. Biol. Chem. 1983;258:11442–11445.
- [3] Fujiki H, Sugimura T. New classes of tumor promoters: teleocidin, aplysiatoxin, and palytoxin. Adv. Cancer Res. 1987;49:223–264.
- [4] Nishizuka Y. Studies and perspectives of protein kinase C. Science. 1986;233:305–312.

- 363 [5] Nishizuka Y. The molecular heterogeneity of protein kinase C and its implications for
364 cellular regulation. *Nature*. 1988;334:661–665.
- 365 [6] Nishizuka Y. Intracellular signaling by hydrolysis of phospholipids and activation of
366 protein kinase C. *Science*. 1992;258:607–614.
- 367 [7] Schaar D, Goodell L, Aisner J, Cui XX, Han ZT, Chang R, Martin J, Grospe S, Dudek L,
368 Riley J, Manago J, Lin Y, Rubin EH, Conney A, Strair RK. A phase I clinical trial of 12-
369 *O*-tetradecanoylphorbol-13-acetate for patients with relapsed/refractory malignancies.
370 *Cancer Chemother. Pharmacol.* 2006;57:789–795.
- 371 [8] Fidler B, Goldberg T. Ingenol mebutate gel (picato): a novel agent for the treatment of
372 actinic keratoses. *P. T.* 2014;39:40–46.
- 373 [9] Pettit GR, Herald CL, Doubek DL, Herald DL, Arnold E, Clardy J. Isolation and structure
374 of bryostatin 1. *J. Am. Chem. Soc.* 1982;104:6846–6848.
- 375 [10] Szállási Z, Smith CB, Pettit GR, Blumberg PM. Differential regulation of protein kinase C
376 isozymes by bryostatin 1 and phorbol 12-myristate 13-acetate in NIH 3T3 fibroblasts. *J.*
377 *Biol. Chem.* 1994;269:2118–2124.
- 378 [11] Szállási Z, Denning MF, Smith CB, Dlugosz AA, Yuspa SH, Pettit GR, Blumberg PM.
379 Bryostatin 1 protects protein kinase C- δ from down-regulation in mouse keratinocytes in
380 parallel with its inhibition of phorbol ester-induced differentiation. *Mol. Pharmacol.*
381 1994;46:840–850.
- 382 [12] Wang QJ, Bhattacharyya D, Garfield S, Nacro K, Marquez VE, Blumberg PM.
383 Differential localization of protein kinase C δ by phorbol esters and related compounds
384 using a fusion protein with green fluorescent protein. *J. Biol. Chem.* 1999;274:37233–
385 37239.
- 386 [13] Lu Z, Hornia A, Jiang YW, Zang Q, Ohno S, Foster DA. Tumor promotion by depleting
387 cells of protein kinase C δ . *Mol. Cell. Biol.* 1997;17:3418–3428.
- 388 [14] Reddig PJ, Dreckschmidt NE, Ahrens H, Simsiman R, Tseng CP, Zou J, Oberley TD,
389 Verma AK. Transgenic mice overexpressing protein kinase C δ in the epidermis are
390 resistant to skin tumor promotion by 12-*O*-tetradecanoylphorbol-13-acetate. *Cancer Res.*
391 1999;59:5710–5718.
- 392 [15] Jackson D, Zheng Y, Lyo D, Shen Y, Nakayama K, Nakayama KI, Humphries MJ,
393 Reyland ME, Foster DA. Suppression of cell migration by protein kinase C δ . *Oncogene.*
394 2005;24:3067–3072.
- 395 [16] Etcheberrigaray R, Tan M, Dewachter I, Kuiperi C, Van der Auwera I, Wera S, Qiao L,

- 396 Bank B, Nelson TJ, Kozikowski AP, Van Leuven F, Alkon DL. Therapeutic effects of PKC
397 activators in Alzheimer's disease transgenic mice. Proc. Natl. Acad. Sci. USA.
398 2004;101:11141–11146.
- 399 [17] Gustafson KR, Cardellina JH, McMahon JB, Gulakowski RJ, Ishitoya J, Szallasi Z, Lewin
400 NE, Blumberg PM, Weislow OS. A nonpromoting phorbol from the Samoan medicinal
401 plant *Homalanthus nutans* inhibits cell killing by HIV-1. J. Med. Chem. 1992;35:1978–
402 1986.
- 403 [18] Wender PA, Verma VA, Paxton TJ, Pillow TH. Function-oriented synthesis, step economy,
404 and drug design. Acc. Chem. Res. 2008;41:40–49.
- 405 [19] Kraft MB, Poudel YB, Kedei N, Lewin NE, Peach ML, Blumberg PM, Keck GE.
406 Synthesis of a des-B-ring bryostatin analogue leads to an unexpected ring expansion of the
407 bryolactone core. J. Am. Chem. Soc. 2014;136:13202–13208
- 408 [20] Nakagawa Y, Yanagita RC, Hamada N, Murakami A, Takahashi H, Saito N, Nagai H, Irie
409 K. A simple analogue of tumor-promoting aplysiatoxin is an antineoplastic agent rather
410 than a tumor promoter: development of a synthetically accessible protein kinase C
411 activator with bryostatin-like activity. J. Am. Chem. Soc. 2009;131:7573–7579.
- 412 [21] Hanaki Y, Kikumori K, Ueno S, Tokuda H, Suzuki N, Irie K. Structure–activity studies at
413 position 27 of aplog-1, a simplified analog of debromoaplysiatoxin with anti-proliferative
414 activity. Tetrahedron. 2013;69:7636–7645.
- 415 [22] Höfle G, Bedorf N, Gerth K, Reichenbach H, inventor; Biotechnolog Forschung Gmbh,
416 assignee. Epothilone, deren Herstellungsverfahren sowie diese Verbindungen enthaltende
417 Mittel. German Patent DE 4,138,042, 1993 Oct 14.
- 418 [23] Bollag DM, McQueney PA, Zhu J, Hensens O, Koupal L, Liesch J, Goetz M, Lazarides E,
419 Woods CM. Epothilones, a new class of microtubule-stabilizing agents with a taxol-like
420 mechanism of action. Cancer Res. 1995;55:2325–2333.
- 421 [24] Borzilleri RM, Zheng X, Schmidt RJ, Johnson JA, Kim SH, DiMarco JD, Fairchild CR,
422 Gougoutas JZ, Lee FYF, Long BH, Vite GD. A novel application of a Pd(0)-catalyzed
423 nucleophilic substitution reaction to the regio- and stereoselective synthesis of lactam
424 analogues of the epothilone natural products. J. Am. Chem. Soc. 2000;122:8890–8897.
- 425 [25] Hunt JT. Discovery of ixabepilone. Mol. Cancer Ther. 2009;8:275–281.
- 426 [26] Nakagawa Y, Irie K, Nakamura Y, Ohigashi H. The amide hydrogen of (–)-indolactam-V
427 and benzolactam-V8's plays a critical role in protein kinase C binding and
428 tumor-promoting activities. Bioorg. Med. Chem. Lett. 2001;11:723–728.

- 429 [27] Nakagawa Y, Irie K, Masuda A, Ohigashi H. Synthesis, conformation and PKC isozyme
430 surrogate binding of new lactone analogues of benzolactam-V8s. Tetrahedron.
431 2002;58:2101–2115.
- 432 [28] Song L, Servajean V, Thierry J. Aziridines derived from amino acids as synthons in
433 pseudopeptide synthesis. Tetrahedron. 2006;62:3509–3516.
- 434 [29] Inanaga J, Hirata K, Saeki H, Katsuki T, Yamaguchi M. A rapid esterification by means of
435 mixed anhydride and its application to large-ring lactonization. Bull. Chem. Soc. Jpn.
436 1979;52:1989–1993.
- 437 [30] Irie K, Oie K, Nakahara A, Yanai Y, Ohigashi H, Wender PA, Fukuda H, Konishi H,
438 Kikkawa U. Molecular basis for protein kinase C isozyme-selective binding: the synthesis,
439 folding, and phorbol ester binding of the cysteine-rich domains of all protein kinase C
440 isozymes. J. Am. Chem. Soc. 1998;120:9159–9167.
- 441 [31] Sharkey NA, Blumberg PM. Highly lipophilic phorbol esters as inhibitors of specific
442 [³H]phorbol 12,13-dibutyrate binding. Cancer Res. 1985;45:19–24.
- 443 [32] Shindo M, Irie K, Nakahara A, Ohigashi H, Konishi H, Kikkawa U, Fukuda H, Wender
444 PA. Toward the identification of selective modulators of protein kinase C (PKC)
445 isozymes: establishment of a binding assay for PKC isozymes using synthetic C1 peptide
446 receptors and identification of the critical residues involved in the phorbol ester binding.
447 Bioorg. Med. Chem. 2001;9:2073–2081.
- 448 [33] Kishi Y, Rando RR. Structural basis of PKC activation by tumor promoters. Acc. Chem.
449 Res. 1998;31:163–172.
- 450 [34] Ganong BR, Loomis CR, Hannun YA, Bell RM. Specificity and mechanism of protein
451 kinase C activation by *sn*-1,2-diacylglycerols. Proc. Natl. Acad. Sci. USA. 1986;83:1184–
452 1188.
- 453 [35] Kang JH, Chung HE, Kim SY, Kim Y, Lee J, Lewin NE, Pearce LV, Blumberg PM,
454 Marquez VE. Conformationally constrained analogues of diacylglycerol (DAG). Effect on
455 protein kinase C (PK-C) binding by the isosteric replacement of *sn*-1 and *sn*-2 esters in
456 DAG-lactones. Bioorg. Med. Chem. 2003;11:2529–2539.
- 457 [36] Nakagawa Y, Irie K, Nakamura Y, Ohigashi H, Hayashi H. Synthesis and biological
458 activities of indolactone-V, the lactone analogue of the tumor promoter (–)-indolactam-V.
459 Biosci. Biotechnol. Biochem. 1997;61:1415–1417.
- 460 [37] Endo Y, Ohno M, Hirano M, Itai A, Shudo K. Synthesis, conformation, and biological
461 activity of teleocidin mimics, benzolactams. A clarification of the conformational

- flexibility problem in structure—activity studies of teleocidins. *J. Am. Chem. Soc.* 1996;118:1841–1855.
- [38] Irie K, Isaka T, Iwata Y, Yanai Y, Nakamura Y, Koizumi F, Ohigashi H, Wender PA, Satomi Y, Nishino H. Synthesis and biological activities of new conformationally restricted analogues of (–)-indolactam-V: elucidation of the biologically active conformation of the tumor-promoting teleocidins. *J. Am. Chem. Soc.* 1996;118:10733–10743.
- [39] Chai JD, Head-Gordon M. Long-range corrected hybrid density functionals with damped atom-atom dispersion corrections. *Phys. Chem. Chem. Phys.* 2008;10:6615–6620.
- [40] zur Hausen H, Bornkamm GW, Schmidt R, Hecker E. Tumor initiators and promoters in the induction of Epstein—Barr virus. *Proc. Natl. Acad. Sci. USA.* 1979;76:782–785.
- [41] Ito Y, Yanase S, Fujita J, Harayama T, Takashima M, Imanaka H. A short-term in vitro assay for promoter substances using human lymphoblastoid cells latently infected with Epstein-Barr virus. *Cancer Lett.* 1981;13:29–37.
- [42] Davies AH, Grand RJ, Evans FJ, Rickinson AB. Induction of Epstein-Barr virus lytic cycle by tumor-promoting and non-tumor-promoting phorbol esters requires active protein kinase C. *J. Virol.* 1991;65:6838–6844.
- [43] Kikumori M, Yanagita RC, Tokuda H, Suzuki N, Nagai H, Suenaga K, Irie K. Structure-activity studies on the spiroketal moiety of a simplified analogue of debromoaplysiatoxin with antiproliferative activity. *J. Med. Chem.* 2012;55:5614–5626.
- [44] Yamori T, Matsunaga A, Sato S, Yamazaki K, Komi A, Ishizu K, Mita I, Edatsugi H, Matsuba Y, Takezawa K, Nakanishi O, Kohno H, Nakajima Y, Komatsu H, Andoh T, Tsuruo T. Potent antitumor activity of MS-247, a novel DNA minor groove binder, evaluated by an in vitro and in vivo human cancer cell line panel. *Cancer Res.* 1999;59:4042–4049.
- [45] Monks A, Scudiero D, Skehan P, Shoemaker R, Paull K, Vistica D, Hose C, Langley J, Cronise P, Vaigro-Wolff A, Gray-Goodrich M, Campbell H, Mayo J, Boyd M. Feasibility of a high-flux anticancer drug screen using a diverse panel of cultured human tumor cell lines. *J. Nat. Cancer Inst.* 1991;83:757–766.
- [46] Sakuma M. Probit Analysis of Preference Data. *Appl. Entomol. Zool.* 1998;33:339–347.
- [47] van der Spoel D, Lindahl E, Hess B, Groenhof G, Mark AE, Berendsen HJC. GROMACS: fast, flexible, and free. *J. Comput. Chem.* 2005;26:1701–1718.
- [48] Wang J, Wang W, Kollman PA, Case DA. Automatic atom type and bond type perception in molecular mechanical calculations. *J. Mol. Graph. Model.* 2006;25:247–260.

- 495 [49] Hanwell MD, Curtis DE, Lonie DC, Vandermeersch T, Zurek E, Hutchison GR.
496 Avogadro: an advanced semantic chemical editor, visualization, and analysis platform. J.
497 Cheminform. 2012;4:17.
- 498 [50] Frisch MJ, Trucks GW, Schlegel HB, Scuseria GE, Robb MA, Cheeseman JR, Scalmani G,
499 Barone V, Mennucci B, Petersson GA, Nakatsuji H, Caricato M, Li X, Hratchian HP,
500 Izmaylov AF, Bloino J, Zheng G, Sonnenberg JL, Hada M, Ehara M, Toyota K, Fukuda R,
501 Hasegawa J, Ishida M, Nakajima T, Honda Y, Kitao O, Nakai H, Vreven T, Montgomery
502 JA, Jr., Peralta JE, Ogliaro F, Bearpark M, Heyd JJ, Brothers E, Kudin KN, Staroverov
503 VN, Kobayashi R, Normand J, Raghavachari K, Rendell A, Burant JC, Iyengar SS,
504 Tomasi J, Cossi M, Rega N, Millam JM, Klene M, Knox JE, Cross JB, Bakken V, Adamo
505 C, Jaramillo J, Gomperts R, Stratmann RE, Yazyev O, Austin AJ, Cammi R, Pomelli C,
506 Ochterski JW, Martin RL, Morokuma K, Zakrzewski VG, Voth GA, Salvador P,
507 Dannenberg JJ, Dapprich S, Daniels AD, Farkas Ö, Foresman JB, Ortiz JV, Cioslowski J,
508 Fox DJ. Gaussian 09. Revision D.01. Wallingford CT: Gaussian, Inc.; 2009.

Table 1. K_i values for the inhibition of [^3H]PDBu-binding by aplog-1, **1**, **2**, and **3**.

	K_i (nM)			
	Aplog-1 ^a	1 ^b	2 ^b	3
δ -C1B peptide	7.4	> 2,500	> 2,500	520 (19) ^c

^a Cited from ref. 20. ^b Cited from ref. 21.

^c Values in parentheses represent the standard deviation from triplicate experiments.

Figure captions

513

514 **Fig. 1.** Structures of bryostatin-1, aplysiatoxin, its simplified analogs (**1-3**), teleocidin-B4,
515 indolactam-V, and its 8-membered analogs.

516

517 **Fig. 2.** Cross-eyed stereo views of possible conformations of **3** (**A-C**) and their relative
518 energies at the ω B97X-D/6-31G* level. Dashed lines represent hydrogen bonding.

519

520 **Fig. 3.** EBV-EA production induced by TPA, aplog-1, **1**, **2**, and **3**.

521 The percentages of EA-positive cells are shown. Sodium *n*-butyrate (4 mM) was added to all
522 samples to enhance the sensitivity of Raji cells. Only 0.1% of cells were positive for EA at 4
523 mM sodium *n*-butyrate. The final concentration of DMSO was 0.4%. Cell viability
524 exceeded 60%. Error bars show the standard error of the mean ($n = 3$). ^aCited from ref. 43.
525 ^bCited from ref. 21.

526

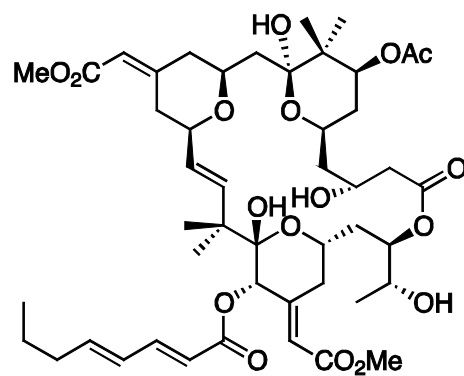
527 **Fig. 4.** Effects of aplog-1, **1**, **2**, and **3** on the growth of human cancer cell lines: HBC-4
528 (breast) and NCI-H460 (non-small cell lung).

529 Cell growth was expressed as a percentage of the control (media only). The results were
530 presented as the average of duplicate points.

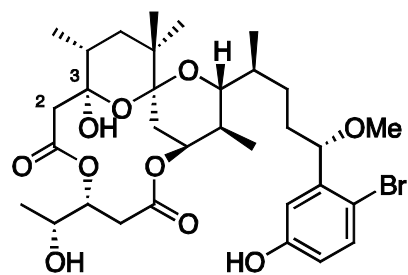
531

532 **Scheme 1.** (a) TFA, dichloromethane (95%); (b) **5**, 2,4,6-trichlorobenzoyl chloride, Et₃N,
533 DMAP, toluene (80%); (c) KMnO₄, NaIO₄, *t*-BuOH, pH 7 buffer (74%); (d)
534 *N*-Hydroxysuccinimide, DCC, MeCN; (e) 20% Pd(OH)₂-C, MeOH (23% in two steps).

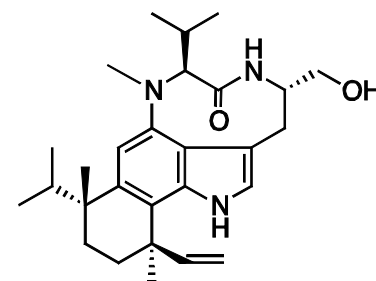
Fig. 1



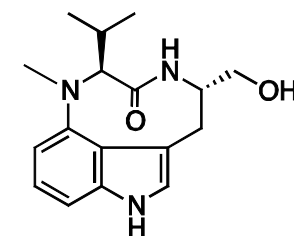
Bryostatin 1



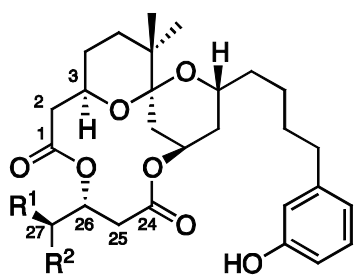
Aplysiatoxin (ATX)



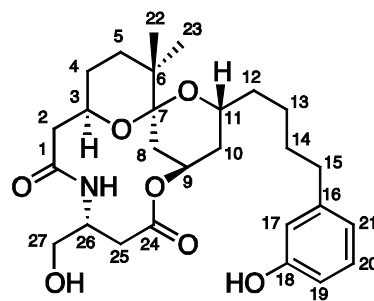
Teleocidin B-4



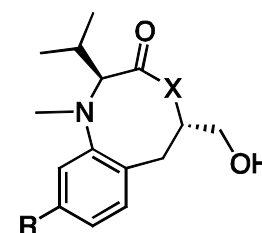
Indolactam-V



Aplog-1 : $R^1 = H$, $R^2 = OH$
1 : $R^1 = Me$, $R^2 = OH$
2 : $R^1 = H$, $R^2 = OMe$



3



Benzolactam-V8s : $X = NH$
 Benzolactone-V8s : $X = O$

Fig. 2

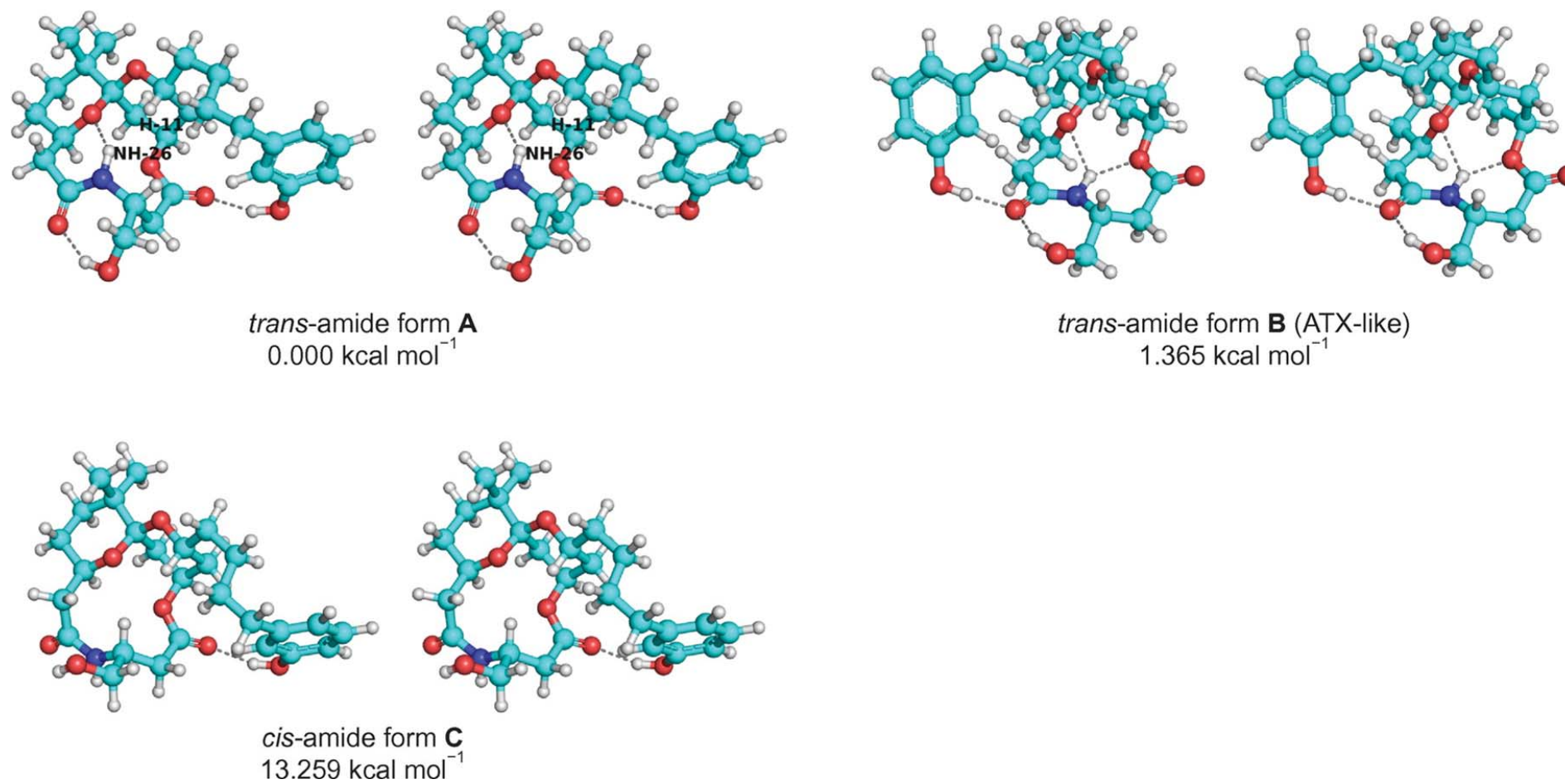


Fig. 3

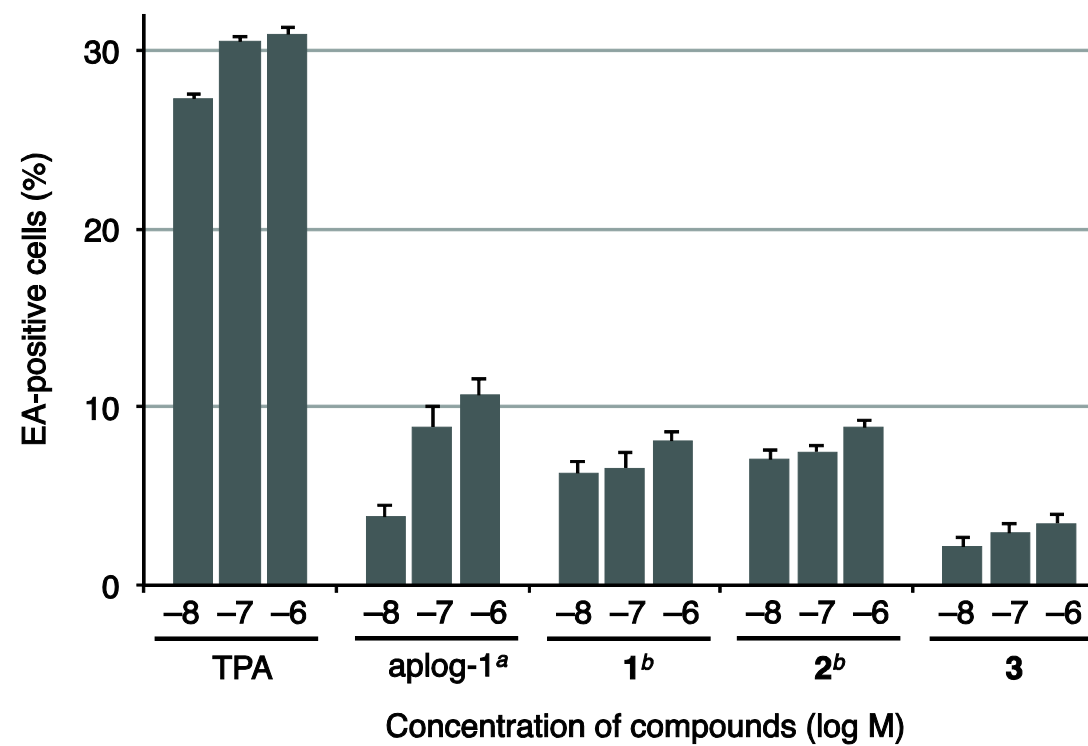
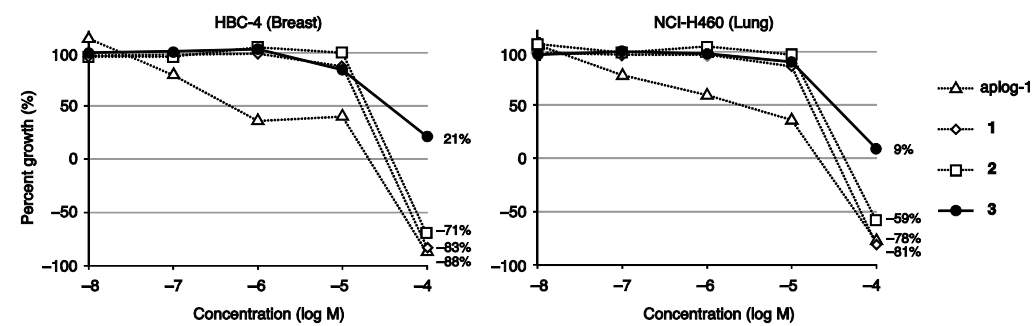
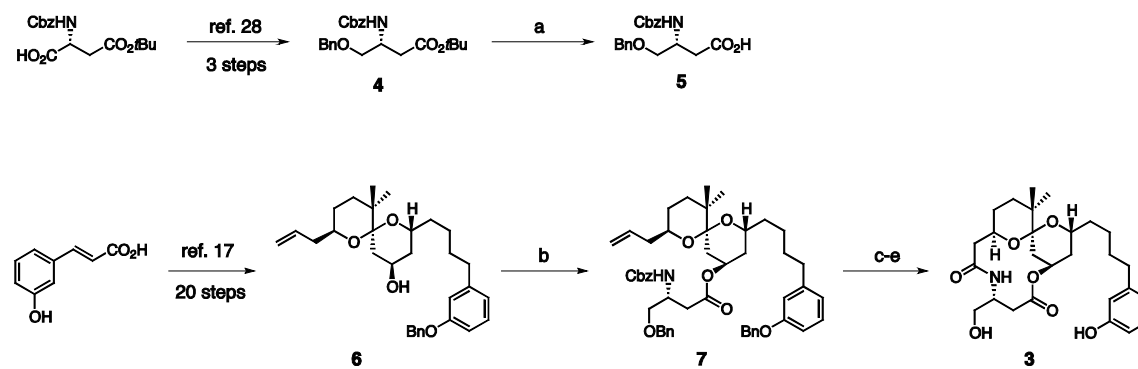


Fig. 4



Scheme1



Supplemental Figures and Table

Synthesis and biological activities of the amide derivative of aplog-1, a simplified analog of aplysiatoxin with anti-proliferative and cytotoxic activities

Yusuke Hanaki,¹ Ryo C. Yanagita,^{1,2} Takahiro Sugahara,³ Misako Aida,³ Harukuni Tokuda,⁴ Nobutaka Suzuki,⁴ and Kazuhiro Irie^{*,1}

¹*Division of Food Science and Biotechnology, Graduate School of Agriculture, Kyoto University, Kyoto 606-8502, Japan*

²*Department of Applied Biological Science, Faculty of Agriculture, Kagawa University, Kagawa 761-0795, Japan*

³*Center for Quantum Life Sciences, and Department of Chemistry, Graduate School of Science, Hiroshima University, Higashi-Hiroshima 739-8526, Japan*

⁴*Department of Complementary and Alternative Medicine, Clinical R & D, Graduate School of Medical Science, Kanazawa University, Kanazawa 920-8640, Japan*

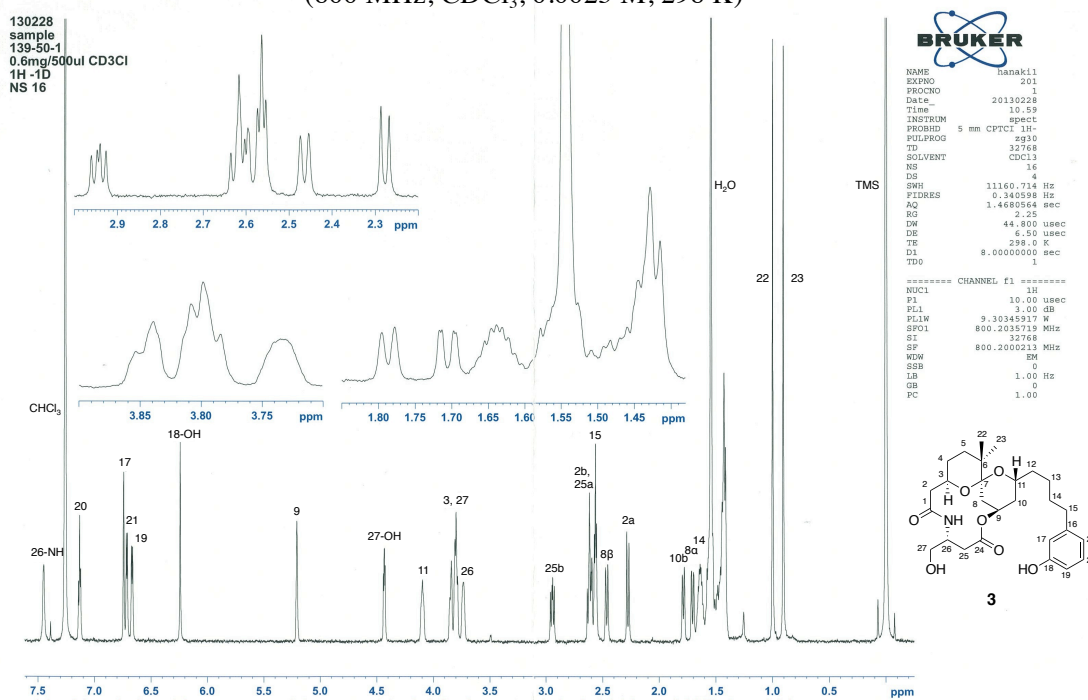
Contents

Supplemental Fig. 1. ¹H-1D NMR spectrum of amide-aplog-1 (3)

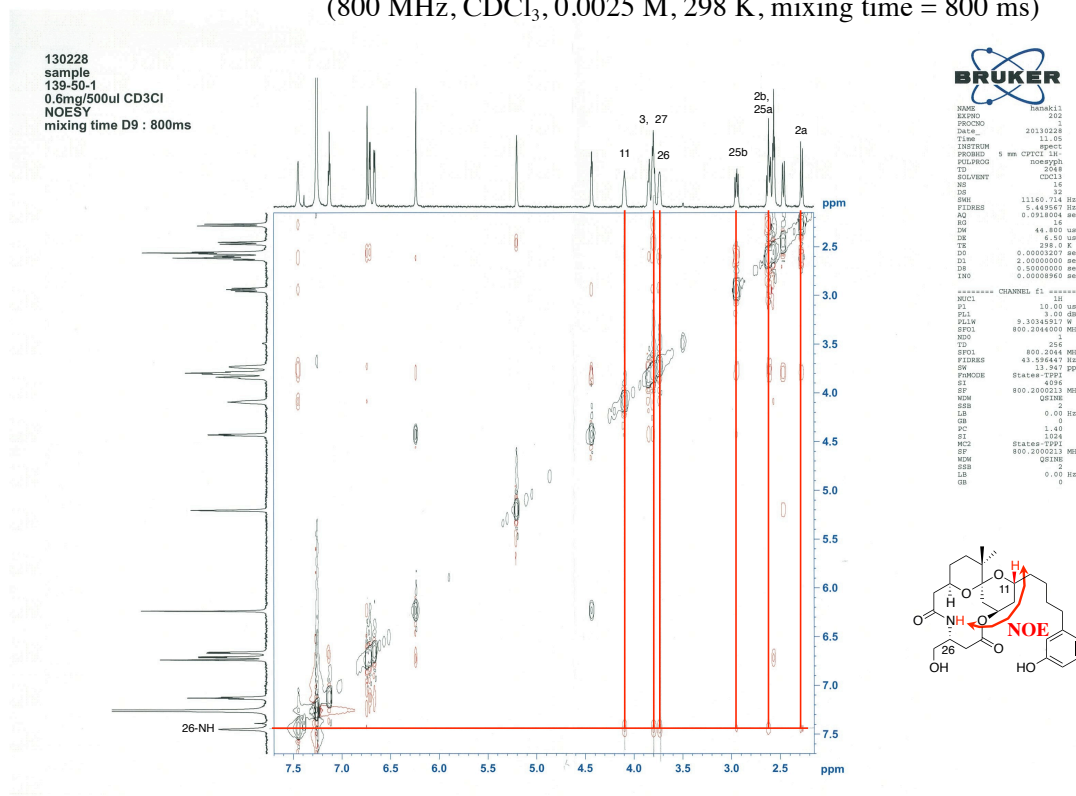
Supplemental Fig. 2. 2D ¹H-¹H NOESY spectrum of amide-aplog-1 (3)

Supplemental Table 1. Growth inhibition assay against human cancer cell lines.

Supplemental Fig. 1. ^1H -1D NMR spectrum of amide-aplog-1 (**3**)
(800 MHz, CDCl_3 , 0.0025 M, 298 K)



Supplemental Fig. 2. 2D ^1H - ^1H NOESY spectrum of amide-aplog-1 (**3**)
(800 MHz, CDCl_3 , 0.0025 M, 298 K, mixing time = 800 ms)



Supplemental Table 1. Growth inhibition assay against human cancer cell lines.

cancer cell line		log GI ₅₀ (M)		Cell growth at 10 ⁻⁴ M (% of control)			
		Aplog-1 ^a	3	Aplog-1	1	2	3
breast	HBC-4	-6.33	-4.46	-88	-83	-71	21
	BSY-1	-4.87	-4.37	-94	-93	-88	27
	HBC-5	-4.76	-4.20	-85	-84	-92	40
	MCF-7	-4.72	-4.50	-82	-72	-80	8
	MDA-MB-231	-5.61	-4.64	-92	-87	-95	9
CNS	U251	-4.83	-4.47	-89	-93	-81	8
	SF-268	-4.83	-4.31	-83	-87	-72	31
	SF-295	-5.06	-4.54	-80	-61	-67	4
	SF-539	-4.97	-4.37	-84	-75	-81	16
	SNB-75	-4.80	-4.39	-84	-81	-70	17
	SNB-78	-4.72	-4.23	-88	-91	-55	38
colon	HCC2998	-5.43	-4.32	-86	-84	-78	22
	KM-12	-4.86	-4.35	-87	-67	-71	24
	HT-29	-4.77	-4.53	-86	-80	-79	-8
	HCT-15	-4.76	-4.31	-75	-67	-46	28
	HCT-116	-4.79	-4.40	-87	-81	-98	16
lung	NCI-H23	-4.88	-4.26	-75	-68	-71	25
	NCI-H226	-4.81	-4.49	-79	-78	-89	9
	NCI-H522	-4.87	-4.65	-88	-87	-89	-25
	NCI-H460	-5.60	-4.50	-78	-81	-59	9
	A549	-5.32	-4.49	-79	-76	-75	9
	DMS273	-4.90	-4.38	-80	-74	-84	16
	DMS114	-4.79	-4.53	-84	-83	-85	3
melanoma	LOX-IMVI	-5.74	-4.73	-83	-70	-91	-62
ovarian	OVCAR-3	-4.78	-4.48	-84	-85	-78	10
	OVCAR-4	-4.75	-4.35	-85	-87	-94	32
	OVCAR-5	-4.95	-4.00	-93	-87	-96	64
	OVCAR-8	-4.71	-4.35	-73	-62	-80	23
	SK-OV-3	-4.69	-4.22	-96	-67	-40	35
renal	RXF-631L	-4.79	-4.29	-91	-88	-77	29
	ACHN	-4.92	-4.46	-92	-97	-28	8
stomach	St-4	-5.55	-4.39	-84	-72	-72	21
	MKN1	-4.86	-4.26	-81	-76	-90	31
	MKN7	-4.78	-4.44	-87	-59	-60	13
	MKN28	-4.74	-4.43	-63	-62	-71	19
	MKN45	-5.33	-4.31	-89	-61	-43	31
	MKN74	-4.76	-4.43	-79	-69	-78	16
prostate	DU-145	-4.85	-4.29	-86	-68	-62	31
	PC-3	-4.96	-4.41	-65	-69	-56	21
MG-MID ^b		-4.98	-4.40				

^a Nakagawa, Y.; Yanagita, R. C.; Hamada, N.; Murakami, A.; Takahashi, H.; Saito, N.; Nagai, H.; Irie, K. *J. Am. Chem. Soc.* **2009**, *131*, 7573-7579.

^b Full panel mean-graph midpoint.